Calibration of Voltage and Current Transducers for DC Railway Systems

Extension of AMPS 2018 paper #1570466046

Calibration of Voltage and Current Transducers for DC Railway Systems

Gabriella Crotti, Antonio Delle Femine, *Member, IEEE*, Daniele Gallo, *Member, IEEE*, Domenico Giordano, Carmine Landi, *Senior Member, IEEE*, Mario Luiso, *Member, IEEE*

Abstract — **To establish a single European railway area, the European Commission requires, by 2019, that energy billings shall be computed on the actual energy consumed. So, in the near future, all the trains shall be equipped with an energy measurement system, whose measurement accuracy should be assessed and periodically re-verified, as required by EN 50463-2. As for every energy and power measuring system, the voltage and current transducers play a crucial role as their accuracy could determine the performance level of the entire measurement chain. To answer to this emerging need, this paper presents a calibration system allowing the accurate testing of DC voltage and current transducers, up to 6 kV and 300 A and up to 10 kHz. It is able to reproduce all the tests prescribed by EN 50463-2, but, in order to characterize the transducers in actual operating conditions, also a series of additional tests can be reproduced using synthetic complex waveforms or even signals acquired on-board trains. The expanded uncertainty (level of confidence 95 %) of the calibration system is 43 µV/V and 24 µA/A at DC and 520 µV/V and 820 µA/A at 10 kHz. Moreover, the calibration of two commercial voltage and current transducers, currently installed in the trains of an Italian operator, is presented.**

Keywords: DC railway system, power and energy measurement, voltage and current transducer, stationary and dynamic metrological characterization

I. Introduction

In recent years, the implementation of efficient, reliable and environmentally friendly transport systems becomes imperative not only to comply with the international agreements on reducing greenhouse gas emissions ([1]-[4]), but also to guarantee liveable conditions in urban areas. Furthermore, in a very competitive context where other transportation modes are considerably improving their environmental performance and the energy costs are steadily increasing, it is crucial that railway transport reduces its energy use while maintaining or enhancing its service quality and capacity, [5], [6].

One of the most important enabling technology for energy efficiency management is the introduction of a continuous energy metering. This provides a precise understanding of consumptions and allows the transition from conventional distance-based billing, to a system based on actual energy measurements. In this context, to establish a single European railway area, the European Commission requires that new energy billing rules in inter-operable railway networks be adopted by 2019 so that all energy bills shall be computed on the actual energy consumed for traction [7], [8]. To this end, all trains must be equipped with an energy measurement function (EMF), whose measurement accuracy shall be assessed and periodically re-verified, as required by EN 50463-2, [9].

For an accurate and reliable knowledge of the energy absorbed/exchanged between the train and the railway grid, is essential to take into consideration the harsh on-board measurement conditions and the frequent non stationary electrical conditions, [2]. So, to assess the metrological reliability of the EMF under real operating conditions, calibration set ups and procedures which go beyond the well-known procedures developed for pure sinusoidal or continuous regimes are required. In addition to the power/energy measurement, the assessment of the power quality could be a valuable tool to foster the efficiency of the whole railway system by "awarding" the good power quality delivered and absorbed. Power quality is a well addressed topic in AC systems and a lot of procedures, algorithms and measurement systems were presented and widely discussed in scientific literature. A less explored research field is the assessment of power quality in DC systems especially with reference to the railway system, [10].

In both the measurement purposes (energy and power quality measurement), the voltage and current transducers play a crucial role and their accuracy could determine the performance level of the whole system [11]-[15]. As a consequence, there is a strong need for a calibration setup able to test wattmeter including voltage and current transducers for DC railway systems in real operating conditions, in order to fulfil the requirements of [9]. To the best of the author knowledge, similar calibration setups have not been developed, yet. This is one of the EMPIR 16ENG04 MyRailS research project [16].

This paper moves a step in this direction presenting a realization of a laboratory calibration system, able to generate up to 6 kV and 300 A, from DC to 10 kHz, with uncertainty lower than 0.1%, in order to assess the metrological performance of voltage and current transducers, employable in the energy measurement in DC railway systems, in actual operating conditions. At the author knowledge, in scientific literature only [16] presents a calibration setup for DC transducers for railway application with similar objectives. However, this system has some limitations, since it works only with current transducers and up to 3 kHz and only some preliminary results are produced.

This work received financial support from the European Metrology Programme for Innovation and Research (EMPIR), 16ENG04 MyRailS project (EMPIR is jointly funded by the EMPIR participating countries within EURAMET and the European Union) and from the University of Campania "Luigi Vanvitelli" (Piano Strategico VALERE - OPEN ACCESS).

G. Crotti, D. Giordano are with the Istituto Nazionale di Ricerca Metrologica (INRIM) Torino, Italy (email: g.crotti@inrim.it, d.giordano@inrim.it)

A. Delle Femine, D. Gallo, C. Landi, M. Luiso are with Department of Engineering, University of Campania "L. Vanvitelli", Aversa (CE), Italy (emails: antonio.dellefemine@unicampania.it, daniele.gallo@unicampania.it, carmine.landi@unicampania.it, mario.luiso@unicampania.it)

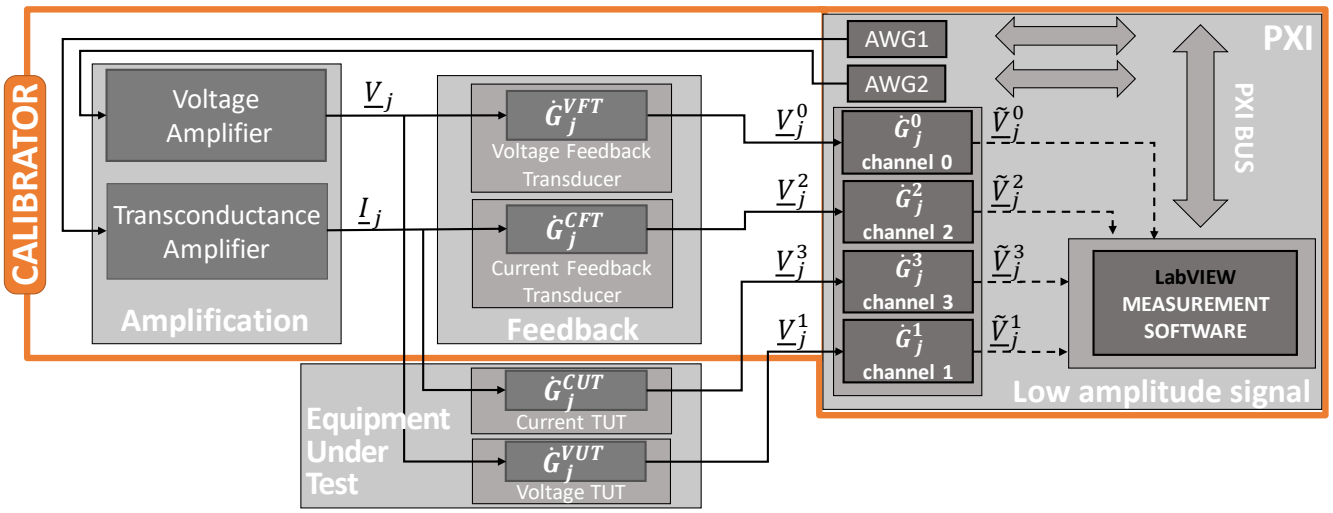

Figure 1. Block diagram of Calibration System

The architecture (see Figure 1.) and basic features of the proposed calibration system has been already presented in [18], [19] showing its ability to generate, in addition to the tests considered in [9], also complex and/or non-stationary test signals, including the possibility to reproduce waveforms acquired on-board trains. In this paper, the calibration system is fully presented with its comprehensive metrological characterization after an accurate evaluation and compensation of all the systematic errors. Its initial capabilities were enhanced with the implementation of new types of tests and, as an example of application, the calibration of two commercial voltage and current transducers, currently installed in the trains of an Italian operator, is presented. In performance verification, also the impact of the operating conditions on the accuracy of the transducers was evaluated. The expanded uncertainty (level of confidence 95 %) of the calibration system is 43 µV/V and 24 µA/A at DC and 520 µV/V and 820 µA/A at 10 kHz. The presented system has the unique feature to perform tests with complex waveforms or with test signals reproducing real field situations. in fact, only DC or sinusoidal calibrations of voltage and current transducers in static conditions are services commonly offered by the National Metrology Institutes. No other characterizations are possible.

The paper is organized as follows. Section II shows a brief review of the actual standard framework about voltage and current transducers for railway systems. Section III is focused on the calibration setup: hardware and software features are discussed and the comprehensive metrological characterization is presented. Section IV presents the experimental results on two commercial voltage and current transducers, currently installed in electrical trains of Trenitalia (the main Italian train operator). Section V discusses the main outcomes of the experimental tests and, finally, Section VI draws the conclusions.

II. Review of Standard Framework

The standard 50463-2 [9], which is focused on energy measuring on-board trains, prescribes that all trains shall be equipped with an EMF, whose measurement accuracy shall be assessed and periodically re-verified. To this end, some accuracy tests are defined for devices devoted to the measurement of the consumed and regenerated active energy of a traction unit. A generic energy measurement system is considered made up of the following functions, which can be contained in one or more devices: Voltage Measurement Function (VMF); Current Measurement Function (CMF); Energy Calculation Function (ECF). In this document, the terms Measurement Function is used as a general term and encompasses the voltage sensor and current sensor that are considered devices implementing measurement functions. For each of these functions, accuracy classes are specified and associated reference conditions are defined. To prove compliance with accuracy class, some basic accuracy tests shall be made for VMF and for CMF. In both cases, some amplitudes are chosen and, under DC reference steady state conditions, the measured error at each measuring point shall be within the prescribed limits. These tests are repeated to verify further deviations due to the influence quantity (temperature, vibrations, etc.).

The only test performed in dynamic conditions is a full scale step response: a step, intended to produce a change in output signal from 0 % to 100 % of the output range, is applied to the input of the sensor. The time for the output to change from 0 % to 90 % of the output range shall be not greater than a specified response time. It is apparent that the described tests are intended to a broad verification of transducers performances and are far from real working conditions (unsteady conditions, large superimposed ripple, etc.). Accuracy or response of transducers in these situations remain untested. So, at the moment, for DC railway systems, there is the lack of a metrological framework (comprising laboratory calibration, measurement set ups and robust data processing algorithms) for calibration of devices as high accuracy energy and power quality meters able to verify the uncertainty limits under highly dynamic electrical conditions.

This document takes a step towards the development of enabling technologies extending the basic test procedures, thus allowing to evaluate the metrological characteristics of the DC voltage and current transducers even in complex conditions, including also real operating conditions.

III. CALIBRATION SYSTEM

A. Hardware and Software Features

A simplified block diagram of the calibration system is reported in Figure 1. and it can be divided into four sections composed by a series of subsystems.

The section with low amplitude signals: this is a PXI (PCI eXtension for Instrumentation) system with two generation boards (National Instruments NI PXI 5422, maximum sampling rate 200 MHz, 16 bit, variable output gain and offset, 256 MB of on-board memory) and one acquisition board (DAQ, NI PXI 4462, input range ± 10 V, 24 bit, sampling rate up to 204.8 kHz).

The amplification section is composed by a transconductance amplifier (Fluke 52120 A, up to 120 A, up to 10 kHz, up to three in parallel) and by a high-voltage power amplifier (NF HVA4321, up to 10 kV, from 0 Hz up to 30 kHz) for current and voltage respectively.

The feedback section is made with two reference transducers used to provide the generated waveforms to the acquisition boards for comparison: Ohm-LABS KV-10A resistive-capacitive voltage divider (10 kV / 10 V) and Ohm-LABS CS-300 current shunt (300 A/30 mV). In the following, they will be referred to as, respectively, Voltage Feedback Transducer (VFT) and Current Feedback Transducer (CFT); the reason for this choice will be clarified in section III.D.

The generated voltage and current waveforms are connected to both feedback transducers and Transducers Under Tests (TUT): their outputs are simultaneously sampled by the DAQ, at a sampling frequency which depends on the frequency content of the generated signals. However, the minimum sampling frequency is 10 kHz.

The measurement software was developed in the LabVIEW environment adopting the state machine approach for managing generation, acquisition and signal processing. Two different operation modes have been implemented:

- In stationary operation mode, the system performs a steady generation of DC voltage and/or current of arbitrary amplitude with the overlapping of a stationary disturbance defined by an arbitrary sum of sinusoidal components (range 0-10 kHz). These tests are aimed to characterize the behaviour also in the presence of harmonic distortion coming from power supply.
- In dynamic operation, the system generates voltage and/or current with time varying DC amplitude that can be defined by user or derived by real signals obtained from experimental data. These tests are intended to characterize the behaviour with the signals that could be found in a real operating conditions. Current and voltage generations and acquisitions are synchronized.

B. Measurement Model

The aim of the presented calibration system is to determine the ratio and phase errors of the TUT, along with the related uncertainty. All the systematic errors of the system have to be measured and compensated to reduce the uncertainty budget. Following the Fig. 1, it is possible to build up a mathematical model of the measurement. Focusing on the complex gain of the voltage TUT (VUT), evaluated at j-th spectral component, equation (1) can be written:

$$\dot{G}_j^{VUT} = \frac{\underline{V}_j^1}{\underline{V}_j} = \frac{\tilde{\underline{V}}_j^1}{\dot{G}_j^1}\frac{\dot{G}_j^{VFT}}{\underline{V}_j^0} = \frac{\tilde{\underline{V}}_j^1}{\tilde{\underline{V}}_j^0}\frac{\dot{G}_j^0}{\dot{G}_j^1}\dot{G}_j^{VFT} \quad (1)$$

where $\dot{G}_j^{VUT}$ ($\dot{G}_j^{VFT}$) is the complex gain of the VUT (VFT), $\underline{V}_j$ is the phasor of the generated voltage, $\underline{V}_j^1$ ($\underline{V}_j^0$) is the phasor of the output of the VUT (VFT), $\dot{G}_j^1$ ($\dot{G}_j^0$) is the complex gain of the channel 1 (channel 0) and $\tilde{\underline{V}}_j^1$ ($\tilde{\underline{V}}_j^0$) is the phasor of the samples at the output of channel 1 (channel 0).

Equation (1) applies for every frequency different from zero. At 0 Hz, all the quantities become real but, in this case, the offset of the DAQ channels must be taken into account. Therefore, equation (1) becomes (2) at 0 Hz.

$$G_0^{VUT} = \frac{\left(\tilde{V}_0^1 + \tilde{O}^1\right)}{\left(\tilde{V}_0^0 + \tilde{O}^0\right)}\frac{G_0^0}{G_0^1}G_0^{VFT} \quad (2)$$

where $\tilde{O}^1$ ($\tilde{O}^0$) is the offset of the channel 1 (channel 0). From (1) and (2) it follows that the systematic errors to be determined are: 1) $\dot{G}_j^0/\dot{G}_j^1$, which is the ratio of the complex gains of the DAQ channels, 2) $\tilde{O}^1$ and $\tilde{O}^0$, which are the offsets of the channels 1 and 0, 3) $\dot{G}_j^{VFT}$, which is the complex gain of the VFT.

Similar equations can be derived also for current transducers. In sections III.C and III.D these systematic errors and the related uncertainty contributions are evaluated.

C. Metrological Characterization of the DAQ

For the measurement of the offsets ($\tilde{O}^0, \tilde{O}^1, \tilde{O}^2, \tilde{O}^3$) of the four DAQ channels, as suggested by the hardware manufacturer, all the inputs have been closed with a 50 Ω termination; then, the input voltages have been acquired, sampling at 200 kHz, and 200,000 points have been averaged. For each channel, all the input ranges (300 mV, 1 V, 3 V, 10 V) have been tested. Each test has been iterated 30 times. Table I shows the voltage offsets and the standard uncertainty for all the channels, for sake of brevity, only for the range ± 300 mV.

As regards the ratios of the complex gains ($\dot{G}_j^0/\dot{G}_j^1$ and $\dot{G}_j^2/\dot{G}_j^3$), they have been measured from 0 Hz to 10 kHz, using the Fluke 5730A calibrator for the generation of the reference signal [20]. More details on this procedure can be found in [21].The same signal has been simultaneously acquired by the four channels. Several tests, accounting different signal amplitudes and different input ranges for all the channels, have been performed. As for the involved frequencies, the channels were tested with a DC value and with sinusoidal signals performing a frequency sweep from 47 Hz to 9870 Hz with linear spacing and 210 frequency steps. The 50 Hz frequency was avoided to minimize interference with the supply power system. In order to obtain a coherent sampling, the acquisition clock has been synchronized with generation system. Then,

TABLE I – INPUT OFFSET MEASUREMENT FOR THE ACQUISTION CHANNELS.

Channel	*Offset [μV]*	*Standard Uncertainty [μV]*
ai0	25.10	0.04
ai1	7.08	0.03
ai2	2.63	0.03
ai3	-29.39	0.03

TABLE II – RATIO ERRORS AND PHASE DISPLACEMENT BETWEEN THE TWO VOLTAGE CHANNELS AND THE TWO CURRENT CHANNELS.

Source	DC		10 kHz	
	Error	Uncertainty*	Error	Uncertainty*
$\Delta R_{0,1}$ [µV/V]	168	10	327	50
$\Delta\varphi_{0,1}$ [µrad]	-	-	5710	55
$\Delta R_{2,3}$ [µV/V]	247	10	-149	50
$\Delta\varphi_{2,3}$ [µrad]	-	-	-7961	55

*standard uncertainty

spectral analyses were performed on the acquired signals, to evaluate the ratios of the complex gains of the channels. From the ratios of the complex gains, the ratio and phase errors of a pair of channels can be retrieved as in (3), referring to the pair of channels 0 and 1.

$$\Delta R_{0,1} = \left(G_j^0/G_j^1 - 1\right), \qquad \Delta\varphi_{0,1} = \measuredangle\dot{G}_j^0 - \measuredangle\dot{G}_j^1 \qquad (3)$$

Table II shows the systematic ratio and phase errors introduced by the two pairs of channels (0 and 1 for voltage, 2 and 3 for current), along with the standard uncertainty, at DC and 10 kHz.

D. Metrological Characterization of Feedback Transducers

One of the most critical part of the proposed calibration system is the availability of voltage and current transducers with the chosen input ranges (6 kV and 300A) and, at the same time, adequate level of accuracy and of frequency range (lower than 0.1 % up to 10 kHz). To the best of authors knowledge, no devices with such specifications are available on the market. In fact, the VFT and CFT have, respectively, rated accuracies of 0.1 % and 0.03 %, but both are certified to work in DC or at low frequency (i.e. 50 / 60Hz). Therefore, in order to meet the requirement on the frequency range (0.1 % up to 10 kHz), it is necessary to accurately measure and compensate their systematic deviations in gain and phase frequency responses, that are the complex gains $\dot{G}_j^{VSR}$ and $\dot{G}_j^{CSR}$, reported in (1).

The VFT has been characterized by a comparison with the Voltage Reference Transducer (VRT) and the CFT by a comparison with Current Reference Transducer (CRT). The INRIM reference voltage divider [12] (30.000 V/3 V, worst expanded uncertainty 0.02% at 10 kHz) was used as VRT. The Fluke A40B-100A (100 A/800 mV, standard uncertainty 30 µA/A @ 1 kHz and 100 µA/A @ 100 kHz) was used as CRT. The measurement model used for the determination of $\dot{G}_j^{VFT}$ and $\dot{G}_j^{CFT}$ is similar to (1), but now $\dot{G}_j^{VFT}$ and $\dot{G}_j^{CFT}$ are the measurands and the reference quantities are $\dot{G}_j^{VRT}$ and $\dot{G}_j^{CRT}$, that are the complex gains of the VRT and CRT and are known from calibration certificates.

The signals adopted for the characterization were composed of a DC component at constant amplitude (3 kV and 100 A) with a superimposed sinusoidal tone, with a peak amplitude of 20 % of DC component) and performing a frequency sweep. For these tests the same setup of Figure 1. and the same software adopted for the bandwidth test and described in Section IV.B were used. The obtained results, in terms of gain and phase errors, are reported in Fig. 2 or VFT and in Fig.3 for CFT. Figure 2 shows a clear low-pass behaviour of the VFT with a – 3 dB cut-off frequency at about 3.6 kHz due to the stray parameters. Instead,

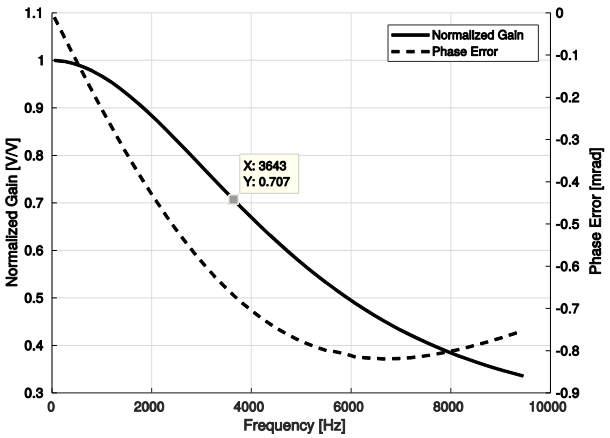

Figure 2. VFT Gain and phase frequency responses.

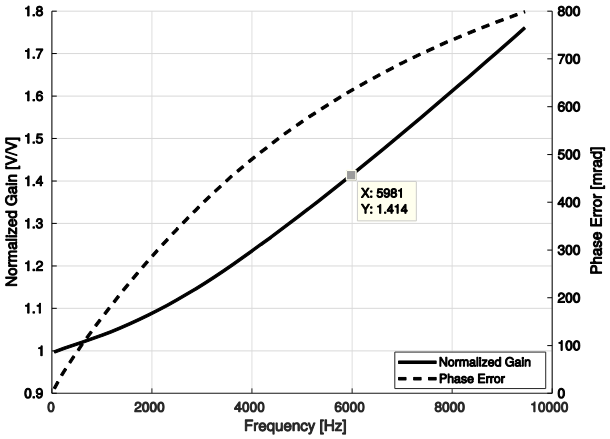

Figure 3. CFT Gain and phase frequency responses

from Figure 3 it is apparent that the CFT, in the considered frequency range, behaves like a high-pass filter due to the skin effect that increases the resistance with frequency.

The measured complex gains $\dot{G}_j^{VFT}$ and $\dot{G}_j^{CFT}$, as shown in Fig. 2 and Fig. 3, are accounted in (1) and (2), in all the working conditions. The expanded uncertainties of systematic ratio and phase errors, as in (3), of VFT and CFT are reported in Table III.

From the analysis of the results in Sec. III.C and III.D, it is apparent that DAQ and feedback transducers become suitable for the presented high performance calibration setup only after the compensation of their systematic errors. In fact, their performances are highly enhanced with the presented procedure of characterization and compensation.

E. Uncertainty Budget

The uncertainty budget is quantified in Table III. It summarizes all the standard uncertainty contributions from the various sources. For simplicity of notation, the uncertainties on ratio errors are reported in part per million (ppm), but voltage ratio errors are expressed in µV/V, whereas those on current in µA/A.

In Table III, the row named “Signal Conditioning” refers to the fact that both the TUTs have current output and a signal conditioning, realized via two Fluke A40B-1A current shunts, is necessary: their standard uncertainties is reported.

TABLE III – UNCERTAINTY BUDGET.

		DC		10 kHz	
Source	**error**	**Voltage**	**Current**	**Voltage**	**Current**
VFT and CFT	**ratio [ppm]**	20	10	250	90
	phase [µrad]	-	-	300	260
Signal Conditioning	**ratio [ppm]**	4.9	4.9	9.5	9.5
	phase [µrad]	-	-	260	260
DAQ	**ratio [ppm]**	5	5	50	50
	phase [µrad]	-	-	55	55
Repeatability & Stability	**ratio [ppm]**	0.1	0.1	5	5
	phase [µrad]	-	-	10	10
Expanded Combined Uncertainty	**ratio [ppm]**	**43**	24	**520**	**210**
	phase [µrad]	**-**	**-**	**820**	**750**

The last row of Table III reports the expanded uncertainty (level of confidence 95 %) of the proposed calibration system. It has been obtained by combining all the contributions of Table III, accounting the measurement models in (1) and (2).

Expanded combined uncertainties (level of confidence 95 %) for voltage (current) channel are, respectively, 520 µV/V (210 µA/A) and 820 µrad (750 µrad) on ratio and phase errors. Those values are lower than 0.1 % up to 10 kHz, which is the target uncertainty of the research project [16]. It is worth to underline that the coverage factor has been determined by following the guidelines reported in Annex G of [22].

IV. EXPERIMENTAL RESULTS

The presented system has been adopted for numerous experimental tests but here for sake of brevity only few of them are reported. In this paper, the considered TUTs are two transducers currently adopted in the Italian railway system: the VUT is the LEM LV 100-4000 (4000 V/50 mA, Accuracy 0.9%, linearity <0.1 %) and the CUT is the LEM/ABB CS2000 (2000 A/400 mA, Accuracy < 0.5 %, linearity <0.1 %, Bandwidth DC - 100 kHz). Both the TUTs have a current output signals: therefore, as explained in section III.E, a signal conditioning, realized via two Fluke A40B-1A current shunts, were used.

It is worth to highlight that all the tests described in the following were performed separately for VUT and CUT; however, for specific needing (i.e. Wattmeter characterization), both generations and acquisitions can be performed simultaneously and in a synchronized way.

A. Stationary Test

Stationary tests are intended to perform measurements with a steady generation of DC signals of chosen amplitude with the overlapping of a stationary disturbance defined by an arbitrary sum of sinusoidal components. Nevertheless, the system does not generate immediately the configured waveform. To avoid a too sudden change in the generated amplitude, the system provides an increasing ramp which, starting from zero, reaches the desired value after 1 s. Then, the measurements are performed and the results are stored. Finally, a decreasing ramp takes back the amplitude of the generated signal to zero. An example of soft start and soft stop adopted for stationary generation is reported in Figure 4.

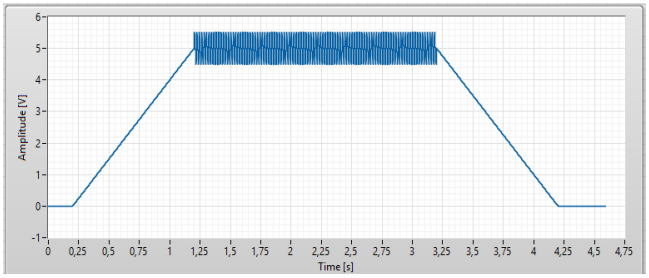

Figure 4. Example of soft start and soft stop of generation

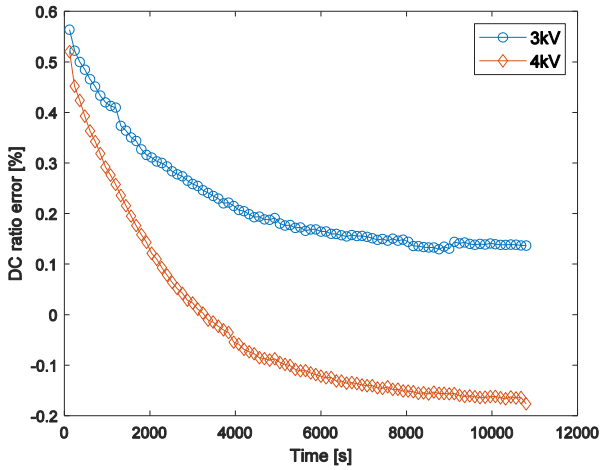

Figure 5. Voltage DC Ratio error versus time of VUT

Results reported in Figure 5. refer to the VUT ratio error, defined as in (3), when it measures a simple DC voltage without any disturbance. It is apparent a remarkable effect of the self-heating of the VUT on its gain: only after 3 hours the considered transducer reaches a steady state. Moreover, the level of the applied voltage makes the phenomenon larger reaching a deviation of 0.7 % for 4 kV. As regards the final level of the ratio error, there is a difference of 0.3 % depending on the amplitude of the continuous component. This strong dependence of the ratio error on the thermal conditions directly impacts on the energy measurement, determining and accuracy that varies with time and environmental conditions. Tests similar to those conducted for the voltage were also conducted for the current. In this case, heating produces far less significant effects and the transducer rapidly reaches the steady state. Also in this case, the ratio error is influenced by the amplitude of the continuous component. Results are not here reported for sake of brevity.

B. Bandwidth Test

A second type of test was performed generating a steady DC voltage at constant value (3 kV) with a single superimposed sinusoidal component with a constant amplitude (i.e. 20 %) but at different frequencies (from 47 Hz till 9870 Hz with a step of 47 Hz). To this aim, a generation frequency of 5 MHz and a sampling frequency of 200 kHz were adopted. For each signal, at the same time, it is possible to evaluate the ratio error, both for DC and AC, and the phase error (only for AC). The measurement of the three parameters was repeated 30 times for each frequency.

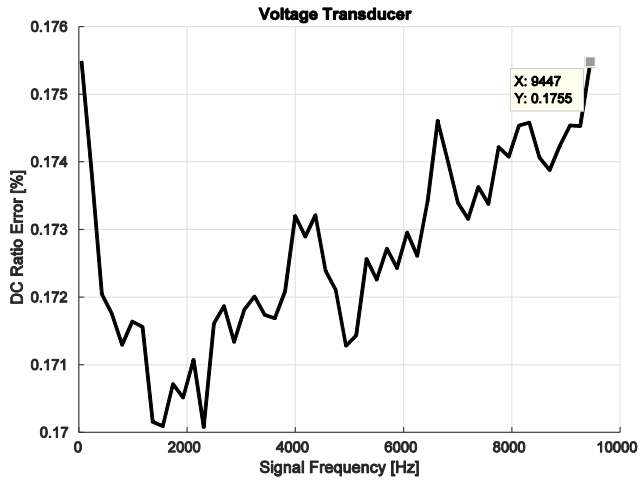

Figure 6. VUT DC Ratio error in presence of sinusoidal distortion

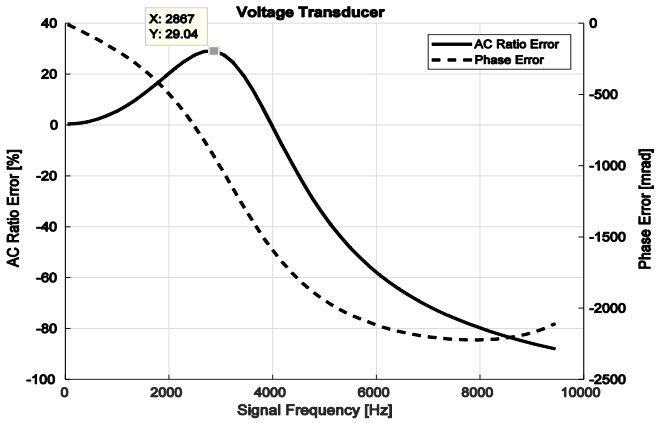

Figure 7. VUT AC ratio and phase errors

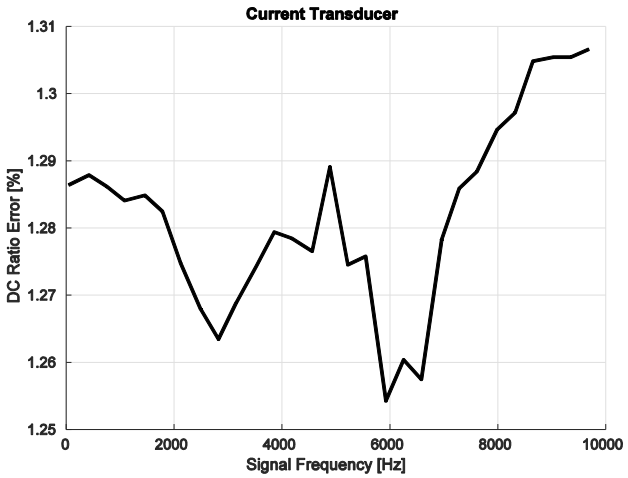

Figure 8. CUT DC Ratio error in presence of sinusoidal distortion

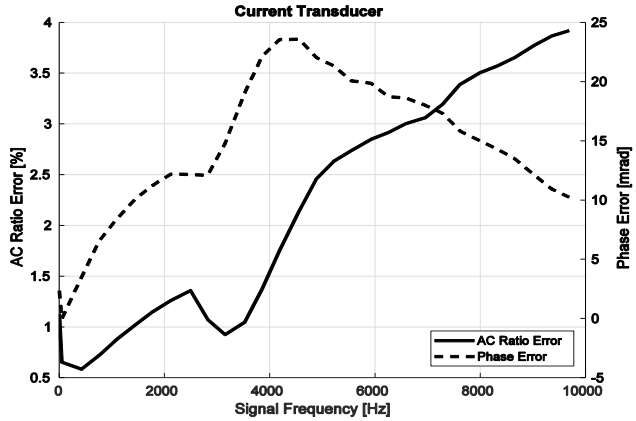

Figure 9. CUT AC Ratio and Phase errors

Figure 6 reports the VUT DC ratio error measured in presence of sinusoidal distortion at various frequencies. This parameter is unaffected by the presence of the sinusoidal component. Figure 7 reports the VUT AC ratio and phase errors measured on the superimposed sinusoidal components. The system acts as low pass filter with resonance frequency slightly lower than 3 kHz. These tests were repeated also with different DC components (from 2 kV to 5 kV with step of 500 V) with substantially identical results so it is possible to conclude that the sinusoidal component does not affect the DC accuracy and the DC component amplitude does not affect the AC frequency response.

The result in Figure 6 and Figure 7 are similar tho those presented in [18]. However the two set-up configurations for voltage calibration have a substantial difference: in [18] the VFT was the INRIM reference divider (here adopted as VRT). The results are similar just because the compensation techniques work properly and all systematic deviations are compensated.

Similar tests were performed also for CUT. Signals with a DC component (300 A) and a single super imposed sinusoidal tone with constant amplitude (i.e. 30 % of DC component) and variable frequency (i.e. 47 Hz to 9870) have been used. Figure 8 reports the CUT DC ratio error measured in presence of sinusoidal distortion at various frequencies. Also in this case, this parameter is substantially unaffected by the presence of the sinusoidal component. Figure 9 reports the CUT AC ratio and phase errors measured on superimposed sinusoidal components. AC ratio error increases almost linearly with frequency presenting a high pass behaviour.

C. Dynamic Tests Derived from Field Measurements

One of the most noteworthy features of the presented system is the capability of reproducing also dynamic working conditions. To this aim, the test system was designed and implemented to be able to reproduce a piecewise sequence of linear behaviours. As first possibility, the user can describe the desired signal in terms of time segments that will be consecutively generated. The k-th segment starting at instant Tk is completely defined assigning its duration, D_k, and the parameters A_k and B_k that define the linear behaviour inside the segment:

$$Y(t) = A_k \cdot (t - T_k) + B_k \qquad for\ t\epsilon[T_k, T_k + D_k] \quad (1)$$

Note that a value for A equal to zero corresponds to a constant behaviour and B_{k+1} equals to the last value of previous segment T_k ($B_{k+1} = A_k D_k + B_k$) assures waveform continuity across the segments. In addition to the manual definition of time segments, a specific procedure was developed to analyse signals coming

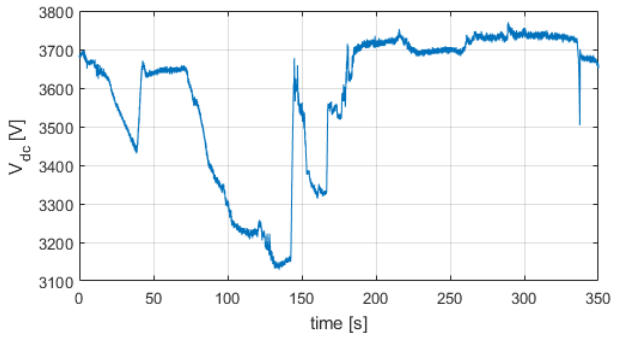

Figure 10. Measured supply voltage of E412

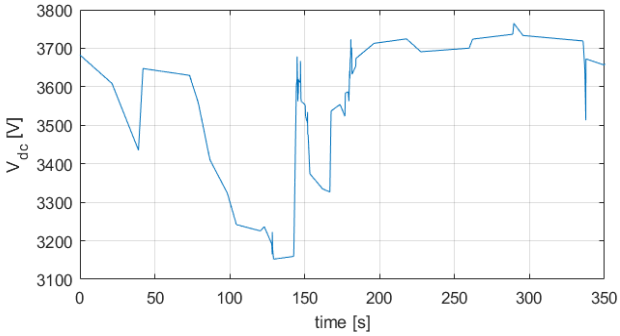

Figure 11. Emulated supply voltage of E412 at 1%

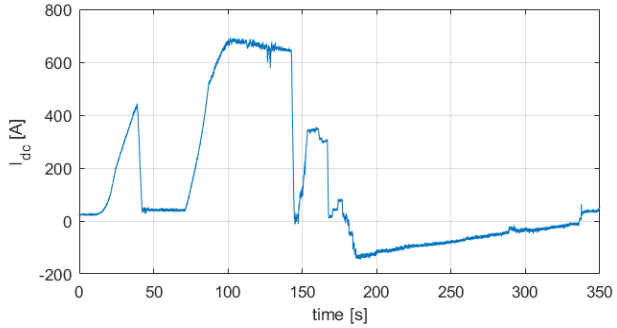

Figure 12. Measured absorbed Current of E412

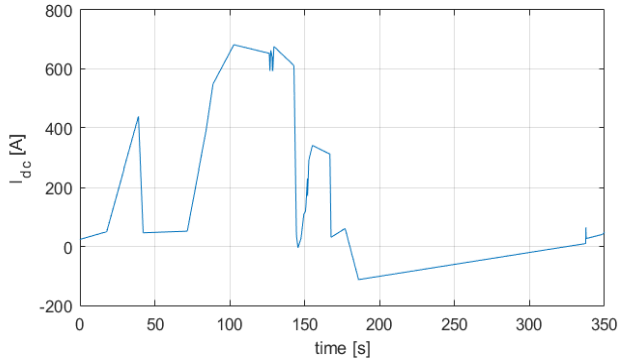

Figure 13. Emulated absorbed Current of E412 at 1.5%

from a field acquisition and to extract their main features to reproduce linearly, during the time, the DC level of voltage or current, within a chosen accuracy. For this aim, the analysed signal is segmented in time intervals in which the time behaviour can be approximated with a linear function, respecting the accuracy limit, and the corresponding parameters are calculated.

The algorithm works analysing a time segment of signal with a first attempt duration (f.i. D_k=1 s) and it exploits the linear least squares fitting for calculating the A_k and B_k parameters. The values obtained with these parameters are compared with the real sample values calculating the maximum deviation. If it is below the chosen tolerance, the algorithm continues to try to extend the duration of the segment (f.i. +10%) and to repeat the estimation of the parameters until the tolerance is exceeded. The values obtained at previous step are stored as final results. If, at the first attempt, the check of tolerance goes wrong, the algorithm continues to decrease the duration of the segment (f.i. -10 %) and to repeat the estimation of the parameters till the tolerance is reached. Then, in both cases, the algorithm goes to the next segment incrementing the starting point of found duration of considered time segment. In the determination of the following segment, the continuity of the waveform through the segments is imposed as a constraint in order to avoid abrupt changes in amplitude. It is apparent that the number of segments depends on the complexity of the waveform but also it changes with the chosen level of accuracy.

As an example, Figure 10 and Figure 12 show the field acquisitions of supply voltage and absorbed current by E412 Locomotive for 350 s with a sampling frequency of 20 kHz during a test of electrical braking (7 million of samples each). As expected, there are high amplitude variations for current according the different working conditions and, consequently, the voltage has inverse behaviour but with lower amplitude variations. Figure 11 and Figure 13 report the piecewise sequence of lines calculated with the algorithm: for the voltage approximation, to meet the tolerance of 1%, 66 time segments were needed, whereas for the current approximation, to meet the tolerance of 1.5%, 46 time segments were needed.

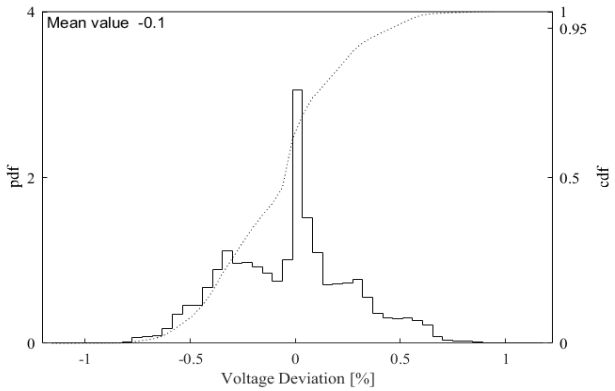

Figure 14. Statistical analysis of deviation in approximating voltage

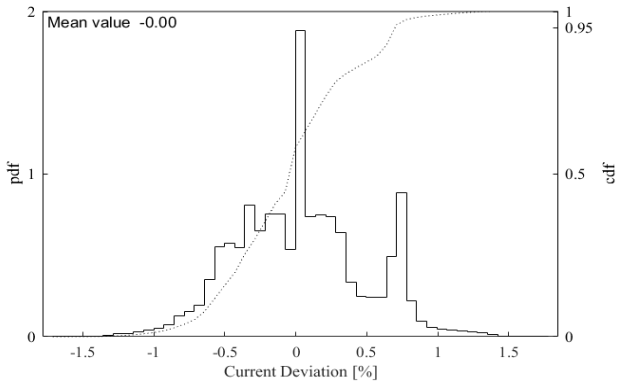

Figure 15. Statistical analysis of deviation in approximating current

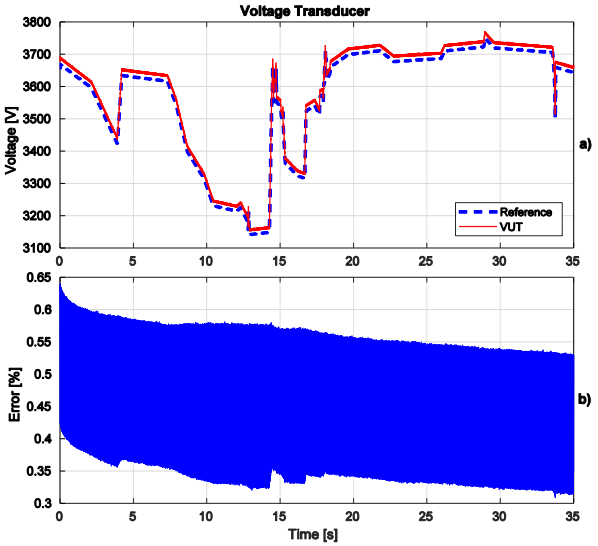

Figure 16. Dynamic test result for voltage and relative error between TUT and reference transducer.

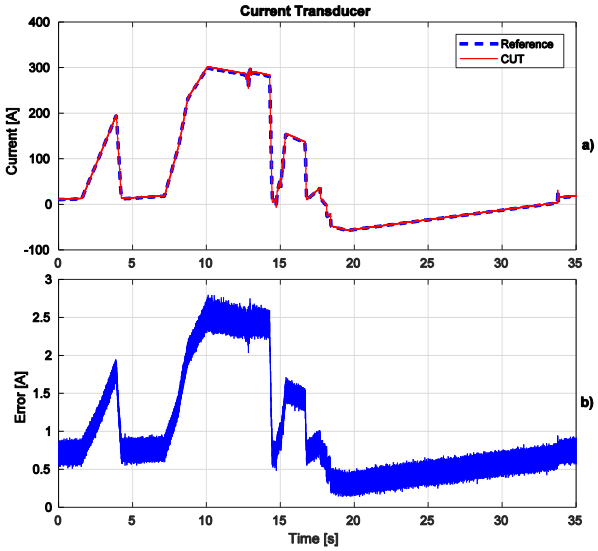

Figure 17. Dynamic test result for current and absolute error between TUT and reference transducer

Obviously, the accuracy limits are the maximum values of deviation found in the considered time segment, but, clearly, the average deviation could be much lower. Figure 14 and Figure 15 report the statistical analyses of all the obtained deviations between the original and the approximated waveforms of voltage and current, respectively.

The obtained coefficients are then processed by a LabVIEW software in order to generate the low voltage signals reproducing a scaled version of the field acquired waveforms. For these test, a generation frequency of 300 A and a sampling frequency of 10 kHz were adopted. These values are consistently lower than those used in the bandwidth tests due to memory allocation problems associated with the high duration of the waveforms.

The adopted approach, as very long time waveforms are defined with few parameters, is particularly suitable for the construction of a test waveform database composed of typical signals that will occur on railway systems, so providing public test cases to which refer for the characterization and the calibration of transducers and measurement devices, that is one of the objective of the research project

The amplitudes of the low voltage signals were calculated accounting voltage and current amplifier gains so that, after amplification, the peaks of signals reach the desired values. For voltage the same peak value of the actual original voltage was reached whereas, for current, the original peak value was reduced till 300 A to meet the transconductance amplifier specifications.

Figure 16a and Fig. 17a show dynamic test results for VUT and CUT, respectively. Both figures show with a dashed line the signal acquired with the reference transducer and with a solid line the same signal acquired with the respective TUT. In Fig. 16b the relative deviation between the VFT and the VUT is

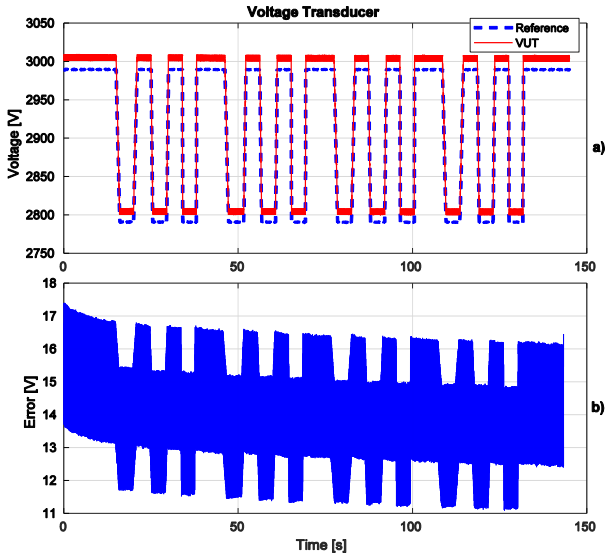

Figure 18. User Defined test result for voltage (a) and absolute error between TUT and reference transducer (b).

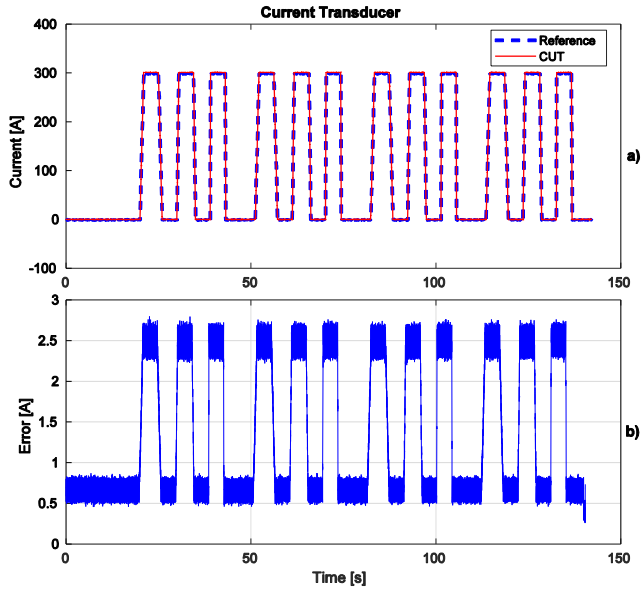

Figure 19. User Defined test result for current (a) and absolute error between TUT and reference transducer (b).

reported, whereas in Fig. 17b the absolute error between CFT and CUT is reported, as current assumes also zero value. From Fig. 16b it is apparent that there is a systematic difference of about +0.45% in the measured voltages nearly independent from measured amplitude with a superimposed noise floor of about ±0.1%. In addition, there is still the presence of thermal drift. The difference in the measurement results of current (see Fig. 18a and Fig. 19a) depend instead on the input current and reach value as high as about 1 %. This is a critical point since determines an accuracy on the measured energy that depends on the operating conditions. The noise has values similar to voltage test, about 0.1 %.

D. User Defined Dynamic Test

In addition to the dynamic tests derived from field measurements, other dynamic tests were implemented with user defined parameters. In particular, the system was configured to generate a sequence of sudden voltage reductions corresponding to current increments (see Fig. 18a and Fig. 19a). These shapes emulate the step test in conditions close to those of the departure and the braking of a locomotive. Three different rise times were implemented (1 s, 0.5 s and 0.1 s) and the chosen amplitude variations were of 300 A and 200 V: the values of amplitudes and rise times are deducted from various field acquisition data (not shown here for sake of brevity). The results in Fig. 18b and Fig. 19b show in a clear way that the accuracy of both the TUTs depends on the amplitude of the input quantity. These test are also intended to analyze the TUT behavior in fast (relative to railway phenomena) transient, f.i. if oscillations are present. The tested TUTs were able to follow the input signal variations even when severe rise time values (0.1 s) are used without any overshot or oscillation.

V. Discussion on Experimental Results

As it is specified in Sec. I, in the very near future, all the trains shall be equipped with energy measuring systems for billing purposes. As it can be seen from real field measurements shown in Sec. IV.C, actual voltage and current waveforms of DC railway systems are very complex (sudden changes, high frequency ripples, slow and fast fluctuations, etc.) and the basic tests proposed by the standard [9] (i.e. stationary DC tests and step tests) can provide only limited indications of the TUT performance. Therefore, the new type of tests presented in this paper goes in the direction of testing the transducers with waveforms as close as possible to the actual conditions. Each of them highlight some important aspects of the transducer's performances that are not evidenced with basic tests required by the actual standard, but which could have remarkable impact on energy measurement. Thus, the presented tests could be a good starting point for the definition of a comprehensive procedure for the transducers calibration that should be defined in the future standards.

With the stationary tests presented in IV.A (Figure 5), the variation of the DC gain of the transducer related to self-heating phenomena is shown. Variations of 0.7 % with time, when the same voltage amplitude is applied, were found. This aspect has a direct impact on voltage and energy measurement: this suggests that this kind of test is significant for TUT performance verification.

The bandwidth tests, discussed in IV.B, aim at showing the performance of the TUTs when spectral components with frequencies different from 0 Hz have to be measured. This is a significant test since due to the power electronics, significant energy exchanges could take place in AC and at higher and higher frequency as a result of the continuous increase of the switching frequency. From the shown experimental results (Fig. 6 to Fig. 9), it is evident that even TUTs with high rated accuracy and bandwidth (that is the CUT with 0.5 % accuracy and 100 kHz bandwidth) have insufficient performance for energy measurement not only at DC (~ 1.27%) but also at higher frequencies (~ 4 % and 23 mrad). Even worse results have been obtained for VUT (~ 0.17 % at DC, in stationary thermal conditions, and ~ 29 % and 2100 mrad at higher frequencies).

As for the "dynamic tests derived from field measurements", discussed in IV.C, they are intended to verify the TUT performance with real field waveforms. It is worthwhile noting that the proposed procedure, for the approximation of real waveforms with piece-wise linear curves, is particularly suitable for the construction of a database of signals derived from real waveforms. It is important to know the behaviour of transducers with those waveforms, for instance because they are common situations waveforms build by this database. It would allow to test transducers in a standardized way close to field working conditions. In particular, the presented waveforms refer to very common working conditions (train starting and braking), and the results obtained (Fig. 16 and Fig. 17) show that TUTs can have performances that depend on the amplitude of input quantities (clearly evident in Fig. 17b) and, moreover, accuracy slightly different from stationary conditions (f.i. for VUT ~ 0.6 % in Fig. 16b instead of ~ 0.17 % in Fig. 6).

Similar considerations can be done also for the experimental results shown in IV.D. In particular, this kind of test gives a clear evidence (Fig. 18b and Fig. 19b) that the accuracy depends on the input quantity amplitude for both the TUTs. Moreover, it can be also useful to determine, with a single test, different performance indices of the TUTs (clearly evident in Figure 19b): the offset (when the input amplitude is zero), the gain (when the input amplitude has the rated value), the rise and fall times and the presence of eventual oscillations in the response.

Summarizing, all the presented results highlight that TUTs, even those with high rated accuracy, can have different behaviours in different test conditions.

This point has a particular importance in the light of the fact that by 2019 all railway energy bills shall be computed on the actual energy consumed for traction, since 1) trains are devices which absorb high amount of energy, 2) the energy cost typically increase with years, 3) all the players of the railway system are strongly interested in the accurate energy measurement and 4) voltage and current transducers are essential devices for the measurement for onboard energy measurement and their performance directly affect the energy measurement.

Therefore, a standard like [9] should address these issues and propose more complex test conditions for accuracy assessment.

VI. Conclusion

This paper presents a calibration system for DC voltage and current transducers for railway applications up to 6 kV and 300 A, with uncertainty of 43 μV/V at DC and 820 μV/V at 10 kHz. It allows to calibrate voltage and current transducers in accordance with the related international standards about energy measurement in railway systems, but it goes far beyond the standard characterization procedures, offering the possibility to test their behaviour with more complex waveforms including test signals acquired on-board trains. The main outcomes of the paper are:

- It presents a unique testbed for the calibration of voltage and current transducers for DC railway system (to the best of the author knowledge no similar setups have been realized).
- It proposed a method to build a high-performance setup starting from commercial voltage and current transducers (VFT and CFT) whose rated accuracies are not sufficient for the scope at hand.
- It shows a procedure for the approximation of real waveforms with piece-wise linear curves, suitable for the construction of a database of signals derived from real waveforms.
- Results of realistic tests for the assessment of the TUT accuracy are presented.
- It is highlighted that future version of the standard [9] should include more complex test conditions to allow a reliable accuracy verification of voltage and current transducers employed for on-board energy measurement.

References

[1] UIC IEA Railway Handbook, “Focus on Passenger Transport. 2017 Edition of the UIC-IEA Railway Handbook on Energy Consumption and CO2 focuses on Passenger Rail Services”, 2017

[2] Bart Van der Spiegel, “Railway Energy Measuring, Managing and Billing” 2009 6th International Conference on the European Energy Market, Pages: 1 - 8

[3] Official Journal of the European Union, Decision No 406/2009/EC on the effort of Member States to reduce their greenhouse gas emissions to meet the Community’s greenhouse gas emission reduction commitments up to 202; 2009.

[4] European Commission, A Roadmap for moving to a competitive low carbon economy in 2050 – Ref. COM(2011) 112 final; 2011

[5] A.González-Gil, R.Palacin, P.Batty, J.P.Powell, “A systems approach to reduce urban rail energy consumption”, Energy Conversion and Management, Vol 80, April 2014, P. 509-524

[6] T. Koseki, “Technologies for saving energy in railway operation: general discussion on energy issues concerning railway technology”, IEEJ Transactions on Electrical and Electronic EngineeringVol. 5, I. 3, May 2010, P. 285-290

[7] Commission Regulation (EU) No 1301/2014 of 18 Nov. 2014 on the technical specifications for interoperability relating to the ‘energy’ subsystem of the rail system in the Union

[8] Commission regulation (EU) No 1302/2014 of 18 November 2014 concerning a technical specification for interoperability relating to the ‘rolling stock — locomotives and passenger rolling stock’ subsystem of the rail system in the European Union

[9] EN 50463-2 – Railway Applications - Energy measurement on board trains - Part 2: Energy measuring

[10] M. Caserza Magro; A. Mariscotti; P. Pinceti, “Definition of Power Quality Indices for DC Low Voltage Distribution Networks”, 2006 IEEE Instrumentation and Measurement Technology Conference Proceedings

[11] G. Crotti; D. Gallo; D. Giordano; C. Landi; M. Luiso; M. Modarres, "Frequency Response of MV Voltage Transformer Under Actual Waveforms", IEEE Transactions on Instrumentation and Measurement, vol. 66, no. 6, pp. 1146-1154, June 2017

[12] G. Crotti, D. Gallo, D. Giordano, C. Landi, M. Luiso, and M. Modarres, M. Zucca, “Frequency Compliance of MV Voltage Sensors for Smart Grid Application”, IEEE Sensors Journal, vol. 17, no. 23, pp. 7621-7629, Dec.1, 1 2017

[13] A. Cataliotti, D. Di Cara, A. E. Emanuel and S. Nuccio, “Current transformers effects on the measurement of harmonic active power in LV and MV networks,” *IEEE Trans. Power Delivery*, vol. 26, no. 1, pp. 360-368, Jan. 2011.

[14] M. Faifer, C. Laurano, R. Ottoboni, S. Toscani and M. Zanoni, "Characterization of Voltage Instrument Transformers Under Nonsinusoidal Conditions Based on the Best Linear Approximation," in IEEE Transactions on Instrumentation and Measurement, vol. 67, no. 10, pp. 2392-2400, Oct. 2018.

[15] A. Mingotti, G. Pasini, L. Peretto and R. Tinarelli, "Effect of temperature on the accuracy of inductive current transformers," 2018 IEEE International Instrumentation and Measurement Technology Conference (I2MTC), Houston, TX, 2018, pp. 1-5.

[16] EURAMET Joint Reaserch Program "Metrology for Smart Energy Management in Electric Railway Systems” 16ENG04 MyRailS

[17] H. E. van den Brom, R. van Leeuwen and R. Homecker, "Characterization of a Reference DC Current Transducer with AC Distortion for Railway Applications," *2018 Conference on Precision Electromagnetic Measurements (CPEM 2018)*, Paris, 2018, pp. 1-2.

[18] G. Crotti ; D. Giordano ; A. Delle Ferninc ; D. Gallo ; C. Landi ; M. Luiso, “A Testbed for Static and Dynamic Characterization of DC Voltage and Current Transducers”, 2018 IEEE 9th International Workshop on Applied Measurements for Power Systems (AMPS) ,26-28 Sept. 2018

[19] A. Delle Femine, D. Gallo, D. Giordano, C. Landi, M. Luiso, R. Visconte “A Set-Up For Static And Dynamic Characterization Of Voltage And Current Transducers Used In Railway Application”, 2018 Journal of Physics Conference Series, 1065(5):052019, September 2018

[20] Fluke 5730A instruction manual, http://download.flukecal.com/pub/literature/5725a__imeng0700.pdf, available online on 28th January 2019.

[21] G. Crotti, D. Gallo, D. Giordano, C. Landi, M. Luiso, “Industrial Comparator for Smart Grid Sensor Calibration”. in IEEE Sensors Journal, vol. 17, no. 23, pp. 7784-7793, 1 Dec.1, 2017.

[22] JCGM 100:2008, “Evaluation of measurement data – Guide to the expression of uncertainty in measurement” (GUM).